International Journal for Innovative Engineering and Management Research
A Peer Revieved Open Access International Journal
www.ijiemr.org

COPY RIGHT

IJIEMR Transactions, online available on 24th July 2017. Link :
http://www.ijiemr.org/downloads.php?vol=Volume-6&issue=ISSUE-5

Title: High Step-Up Dual Switch Converter With Coupled Inductor and Voltage Multiplier For Grid Connected System.

Volume 06, Issue 05, Page No: 2089 – 2099.

Paper Authors

***G.RADHAKRISHNA, M.CHANDRA SHEKHAR, MR. JADAPALLI SREEDHAR.**

* of EEE, Annamacharya Institute of Technology & Sciences.

USE THIS BARCODE TO ACCESS YOUR ONLINE PAPER

To Secure Your Paper As Per UGC Guidelines We Are Providing A Electronic Bar Code

International Journal for Innovative Engineering and Management Research
A Peer Revieved Open Access International Journal
www.ijiemr.org

HIGH STEP-UP DUAL SWITCH CONVERTER WITH COUPLED INDUCTOR AND VOLTAGE MULTIPLIER FOR GRID CONNECTED SYSTEM

[1]G.RADHAKRISHNA, [2]M.CHANDRA SHEKHAR, [3]MR. JADAPALLI SREEDHAR

[1]PG Scholar, Dept of EEE, Annamacharya Institute of Technology & Sciences, Hyderabad, RR (Dt), Telangana, India.

[2]Assistant Professor, Dept of EEE, Annamacharya Institute of Technology & Sciences, Hyderabad, RR (Dt), Telangana, India.

[3]HOD, Dept of EEE, Annamacharya Institute of Technology & Sciences, Hyderabad, RR (Dt); Telangana, India.

ABSTRACT:

A novel high step-up converter, which is suitable for a PV cell is proposed in this paper. The proposed converter is composed of the dual switches structure, the coupled inductor, and voltage multiplier cells in order to achieve the high step-up voltage gain. The dual switches structure is beneficial to reduce the voltage stress and current stress of the switch. In addition, two multiplier capacitors are, respectively, charged during the switch-on period and switch-off period, which increases the voltage conversion gain. Meanwhile, the energy stored in the leakage inductor is recycled with the use of clamped capacitors. Thus, two main power switches with low on-resistance and low current stress are available. As the leakage inductor, diode reverse-recovery problem is also alleviated. Therefore, the efficiency is improved. This paper illustrates the operation principle of the proposed converter; discusses the effect of the leakage inductor; analyzes the influence of parasitic parameters on the voltage gain and efficiency, the voltage stresses and current stresses of power devices; and a comparison between the performance of the proposed converter and the previous high step-up converters is performed. In the ordinary voltage step-up situation, the conventional step-up converters, such as the boost converter can satisfy the voltage step-up requirement. However, in the high step-up situation, the conventional converter cannot achieve a high step-up conversion with high efficiency by extreme duty cycle or high turns ratio because of the parasitic parameters or leakage inductance.

Key Words: Dual switches, high step-up converter, switched capacitor, three-winding coupled inductor, Photo Voltaic System.

I. INTRODUCTION

In recent years, the boost dc/dc converters have been widely used to step up the renewable energy sources in various industrial applications such as ESS, UPS, and EV etc. In those applications, boost dc/dc converters generally step up the voltage to the high voltage output. For that reason, to obtain a high voltage gain, many converter topologies were reported [3]-[6] for this application. Direct

voltage step up using high frequency transformer is a Simple and easily controllable converter providing high gain. Isolated current

International Journal for Innovative Engineering and Management Research
A Peer Revieved Open Access International Journal
www.ijiemr.org

fed dc-dc converters [7]-[9] are example of this category. However, these topologies result in high voltage spikes across the switch (due to leakage inductance) and large ripple in primary side transformer current as the turn's ratio in the high frequency transformer increases. Most

of the non-isolated high voltage gain dc–dc power converters employ coupled inductor (to achieve higher voltage gain) [11] in contrast to a high frequency transformer used by the isolated versions. The coupled inductor-based dc–dc converter has advantages over isolated transformer-based dc–dc converter in minimizing current stress, using lower rating components and simple winding structure. Modeling procedure of the coupled inductor is described in [12]. For high power converter applications, interleaved coupled inductor-based boost converters [13]–[15] have also been proposed. Voltage gain of the converter can be increased without increasing the duty cycle of the switch by connecting an intermediate capacitor in series with the inductor [6]. The intermediate energy storage capacitor with coupled inductor charges in parallel and discharges in series with the coupled inductor secondary.

A demerit of coupled inductor-based systems is that they have to deal with higher leakage inductance, which causes voltage spikes across the main switch during turn-OFF time and current spike during turn-ON time, resulting in a reduction of the overall circuit efficiency. The effects of leakage inductance can be eliminated by using an active clamp network shown in [9], which provides an alternate path to recover leakage energy. But active clamp network is not as efficient as a passive clamp because of conduction losses across the power switch of the active clamp network. Active clamp network consists of a switch with passive components while passive clamp network [4] consists of passive components such as diode, capacitor, and

resistor. The passive clamp circuit is more popular to reduce voltage stress across the converter switch by recycling leakage energy. To overcome such disadvantages of the conventional converters. A closed-loop control system, a sensor monitors the system output and feeds the data to a controller that adjusts the control to maintain the desired system output and hence remain unaffected to the external noise sources. A closed loop control has high reliability, easy implementation and output short circuit and overload protection.

In this paper, we propose coupled inductor boost converter that features low switch voltage stress and high gain. To achieves high voltage through a coupled inductor connected in interleaved manner that charges an intermediate buffer capacitor and a passive clamp network to recover the leakage energy. Coupled inductor leads to the incorporation of "turn's ratio" into the gain expression that leads to high efficiency without increasing the duty ratio. As compared to existing high-gain dc–dc converters, the number of passive components used in the proposed converter is less, which reduces the cost and improves the efficiency. Though the proposed converter is applicable to any low voltage source applications such as solar PV, fuel cell stack, battery, etc. The typical renewable energy system is shown in Fig.1. The system can convert the low voltage from

International Journal for Innovative Engineering and Management Research
A Peer Revieved Open Access International Journal
www.ijiemr.org

the fuel cells source and photovoltaic cells source into the high voltage via the high step-up converter, and, then, the renewable energy is transformed into the load and utility through the inverter. Therefore, the high step-up converter is indispensable.

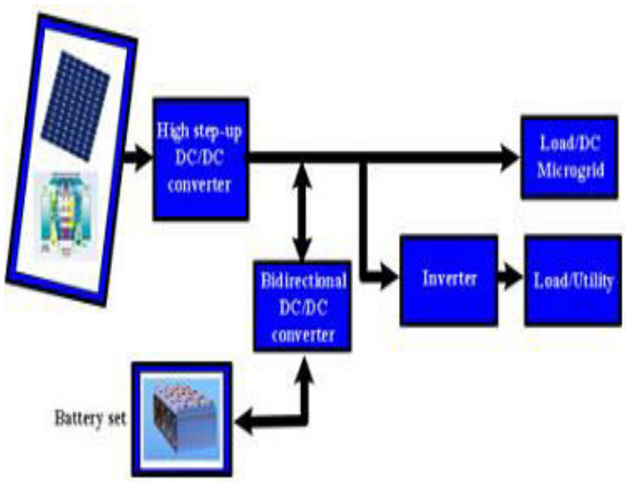

Fig.1. Typical renewable energy system

II. OPERATION PRINCIPLE OF THE DUAL SWITCHES CONVERTER

Fig.2 shows the circuit topology of the proposed converter. The equivalent circuit model of the three-winding coupled inductor includes the magnetizing inductance Lm, the leakage inductance L_k, and an ideal transformer with primary winding N_1 turns and two secondary windings N_2 and N_3 turns. The proposed converter consists of two active switches, five diodes, and five capacitors. The switches S_1 and S_2 share the same operation signal and one control circuit is needed. The leakage inductor energy of the coupled inductor is recycled to the capacitors C_1 and C_2, and the voltage spikes on the switches are significantly reduced. This makes low conducting resistance R_{ds}(on) of the switches available. Thus, the efficiency is upgraded and the high step-up conversion gain can be achieved. Also, the voltages across the capacitors C_3 and C_4 can be adjusted by the turns ratio of the coupled inductor. To simplify the circuit analysis of the proposed converter, the following assumptions are made:

1) The CapacitorsC$_1$, C_2, C_3, C_4, and Co is large enough; thus, V_{C1}, V_{C2}, V_{C3}, V_{C4}, and Vo are regarded as constant values;
2) The power devices are ideal, but the parasitic capacitors of the switches are considered;
3) The coupling coefficient of the coupled inductor k is equal to Lm/ (Lm+Lk), and the turns ratio of the coupled inductor is N_1:N_2:N_3 =1:1:N. The primary winding with N_1 turns, two secondary windings with N_2 and N_3 turns of the ideal transformer with are, respectively, represented by L_1, L_2 and L_3(L_1 :L_2 :L_3 =1:1:N_2).

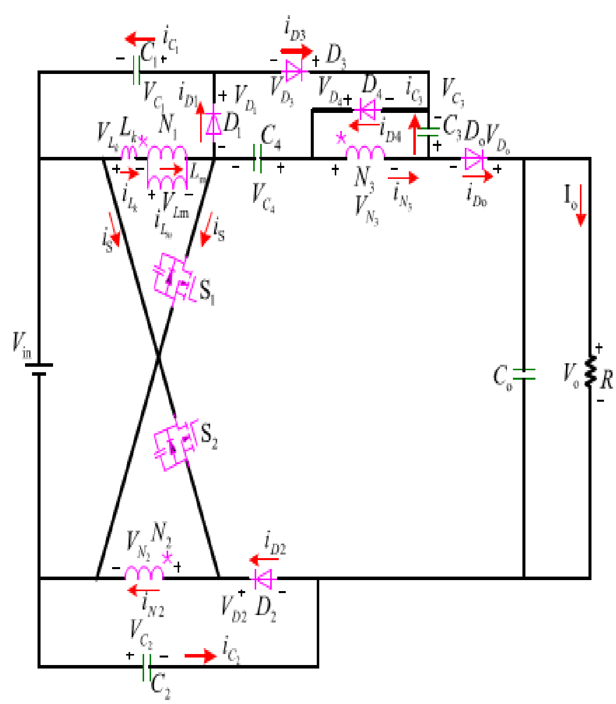
Fig.2. Circuit configuration of the proposed converter

International Journal for Innovative Engineering and Management Research
A Peer Revieved Open Access International Journal
www.ijiemr.org

The operating principles for the continuous conduction mode (CCM) are analyzed in detail herein. Fig.3 shows the typical waveforms of the proposed converter during one switching period. Fig.4 shows the topological stages of the proposed converter.

The eight operating modes are described as follows.

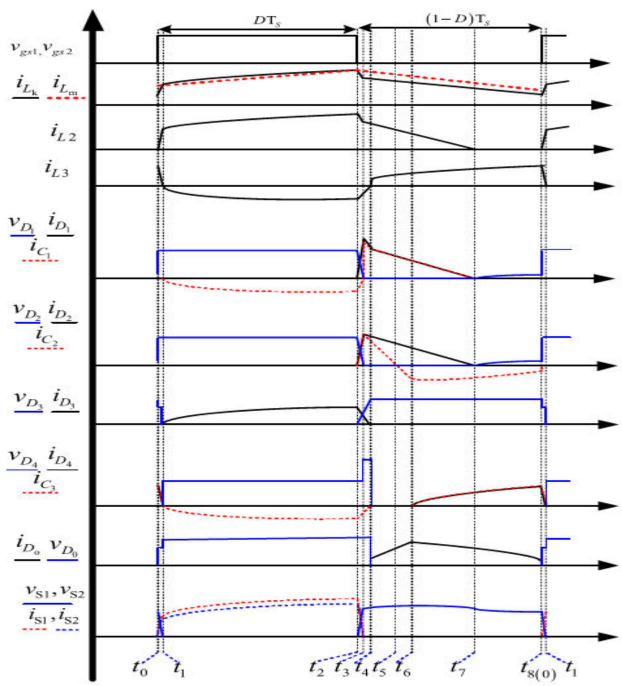

Fig.3. Typical waveforms of the proposed converter during one switching period

A. CCM Operation

Mode I [t_0, t_1]: In this transition interval, the switches S_1 and S_2 start to conduct. Diodes D_1, D_2, D_3, and Do are reverse biased. Diode D_4 is forward biased. The current flow path is shown in Fig.4 (a). The leakage inductance L_k and magnetizing inductance Lm are charged by the input source Vin. The inductor L_2 is also charged by the input source. The leakage inductor current i_{Lk} increases linearly. Due to the leakage inductance, the inductor current i_{L3} and diode current i_{D4} decrease slowly.

Therefore, the voltage of diode D_3 is clamped by input source Vin, clamped voltages V_{C1} and V_{C4}; the voltage of diode Do is clamped by blocking voltagesV_{C3}, V_{C4}, and V_{C2}. The voltage steps are formed. The output capacitor

Co provides the energy to load R. When the current i_{D4} becomes zero (i.e., i_{Lk} =i_{Lm}), this operating mode ends.

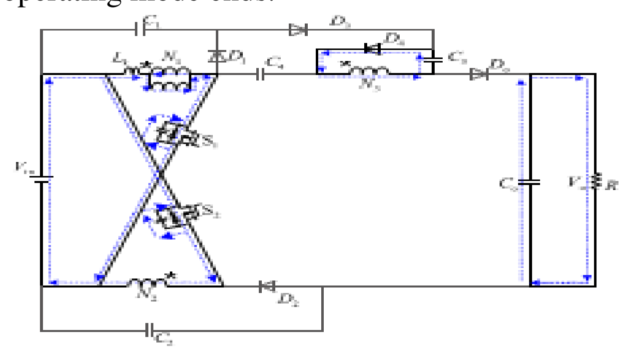

(a)

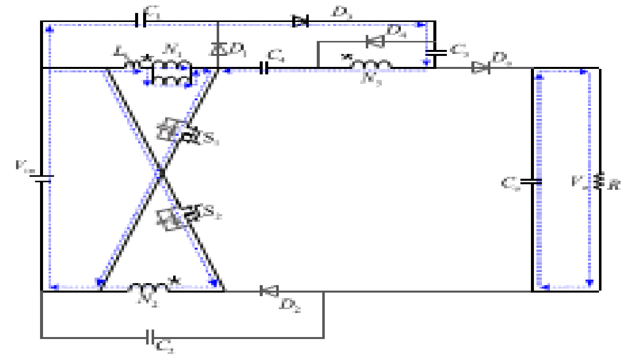

(b)

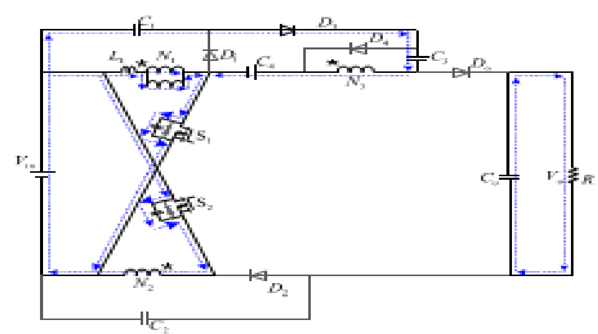

(c)

International Journal for Innovative Engineering and Management Research
A Peer Revieved Open Access International Journal
www.ijiemr.org

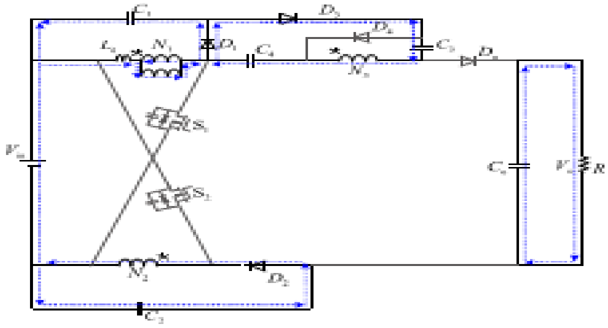

(d)

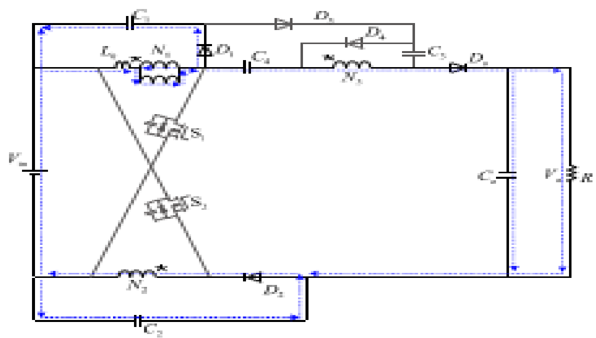

(e)

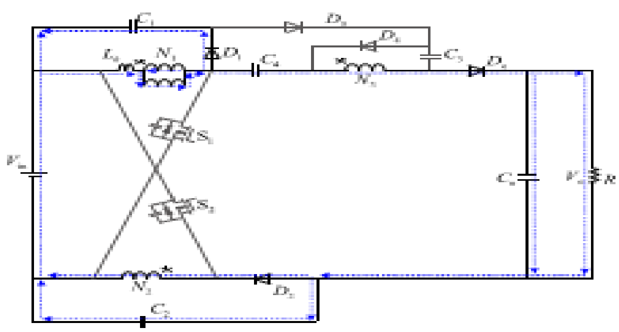

(f)

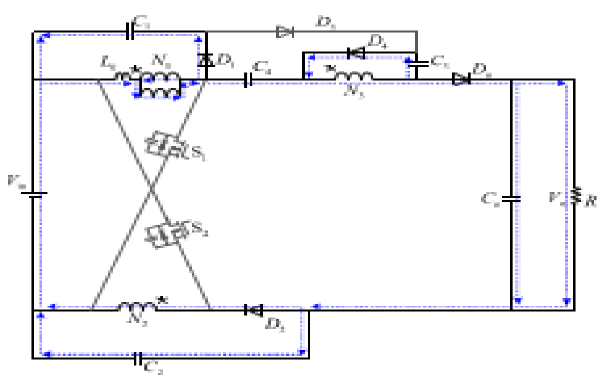

(g)

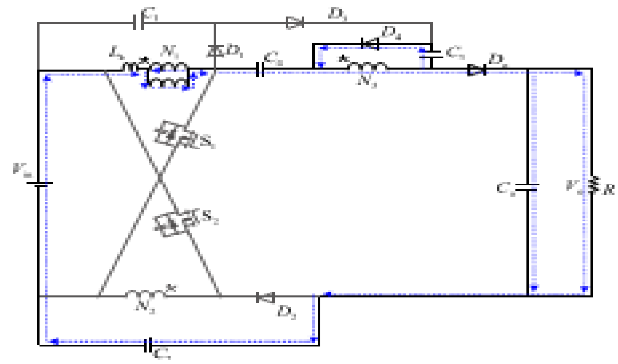

(h)

Fig.4. Equivalent circuit of the proposed converter

Mode II [t_1, t_2]: In this transition interval, the switches are still turned on. Diode D_3 is forward biased. Diodes D_1, D_2, D_4, and Do are reverse biased. The current flow path is shown in Fig.4 (b). The magnetizing inductance Lm and inductor L_2 are charged in parallel by the input source Vin. Some of the energy from the input source Vin transfer to the inductor L_3 to charge blocking capacitor C_4 with the input source Vin, blocking voltages V_{C1}, V_{C3} together. The output capacitor Co provides the energy to load R. When the switches are turned off at t =t_2, this interval is finished.

Mode III [t_2, t_3]: In this transition interval, the switches are turned off. Diodes D_1, D_2, D_4, and Do are reverse biased. Fig.4(c) shows the current-flow path. The energies of the leakage inductance L_k and magnetizing inductance Lm are released to the parasitic capacitors of the switches, respectively. The blocking capacitorC4 is still charged. The output capacitor Co provides the energy to load R. When the diodes D_1 and D_2 are forward biased at t =t_3, this operating mode ends.

Mode IV [t_3, t_4]: In this transition interval, the switches are turned off. Diodes D_1, D_2, and D_3 are forward biased. Diode Do is

International Journal for Innovative Engineering and Management Research
A Peer Revieved Open Access International Journal
www.ijiemr.org

reverse biased. Fig.4 (d) shows the current-flow path. The energies of the leakage inductance L_k and magnetizing inductance Lm are released to the clamped capacitor C_1 and energy of the inductor L_2 is transferred to the clamped capacitor C_2. The blocking capacitor C_4 keeps charging. In addition, due to the leakage inductance, and the diode current i_{D3} keeps flowing though diode D_1; therefore, the voltage across the diode D_4 is clamped by the blocking voltage V_{C4}. The output capacitor Co provides

the energy to load R. When the currents i_{D3}, i_{C3}, and i_{L3} decrease to zero at t =t_4, this operating mode ends.

Mode V [t_4, t_5]: In this transition interval, the switches are turned off. Diodes D_1, D_2, and Do are forward biased. Diodes D_3 and D_4 are reverse biased. The current-flow path is shown in Fig.4 (e). The energies of the leakage inductance L_k and the magnetizing inductance Lm are released to the clamped capacitor $C_1$and the energy of inductor L_2 is transferred to the clamped capacitor C_2. The diode current i_{Do} increases almost at a constant slope. The input source Vin, three-winding coupled inductor, and the blocking voltage V_{C4} are connected in series to charge the output capacitor Co and provide energy to the load R. When the diode current i_{Do} is equal to diode current i_{D2} (i.e., capacitor current decreases to zero) at t =t_5, this operating mode is finished.

Mode VI [t_5, t_6]: In this transition interval, the switches are turned off. Diodes D_1, D_2, and Do are forward biased. Diodes D3 andD4 are reverse biased. The current-flow path is shown in Fig.4 (f). The operating mode is almost the same as Mode V except that the capacitorC2 is discharged instead of charged. When the diodeD4 is forward biased at t =t_6, this operating mode ends.

Mode VII [t_6, t_7]: In this transition interval, the switches are turned off. Diodes D_1, D_2, D_3, and Do are forward biased. Diode D_4 is reverse biased. The current-flow path is shown in Fig.4 (g). The energies of the leakage inductance L_k and the magnetizing inductance Lm are released to the clamped capacitor C_1. The inductor L_2 and the capacitor C_2 are connected in parallel to discharge the energies to the load and the output capacitor Co.

Meanwhile, the input source V_{in}, inductors $L_1$and L_2, as well as the blocking voltage V_{C4} provide energy to the output capacitor Co and the load R. The output diode current i_{Do} drops almost at a constant slope. In addition, the part energy of the inductorL2is transferred to the capacitor C3. When the diode currents i_{D1} and i_{D2} are equal to zero t =t_7, this operating mode ends.

Mode VIII [t_7, t_8]: In this transition interval, the switches are turned off. Diodes D_3 and Do are forward biased. Diodes D_1, D_2, and D_4 are reverse biased. The current-flow path is shown in Fig.4 (h). The leakage inductance L_k, the magnetizing inductance Lm, the input source Vin, the inductor L_3, the blocking voltage V_{C4}, and the clamped capacitor voltage V_{C2} are connected in series to provide energy to the output capacitor Co and the load R. Meanwhile, capacitor C_3 keeps charging.

The voltages across the diodes D_1 and D_2 are clamped by the windings of the coupled inductor and the clamped capacitors C_1 and C_2. Therefore, the voltage steps of diodes D_1 and D_2 are formed, and the voltage drops of the switches are obtained. The output diode current i_{Do} drops linearly. When the output diode Do is

International Journal for Innovative Engineering and Management Research
A Peer Revieved Open Access International Journal
www.ijiemr.org

reverse biased at $t=t_8$, this operating mode ends. When the switches are turned on, the new switching period begins.

III. PERFORMANCE ANALYSIS OF THE PROPOSED CONVERTER

A. Voltage Gain Expression

When the proposed converter operates in the switching-on state, the following equations can be found in Fig.4 (b):

$$V_{L_m} = kV_{in} \tag{1}$$

$$V_{L_k} = (1-k)V_{in} \tag{2}$$

At modes V–VII, the energies of the leakage inductors are released to the capacitors C1 and C2. According to Tang et al, the duty cycle of the released energy can be approximately obtained

$$D_c = 2(1-D)/(N+1) \tag{3}$$

By using the volt–second balance principle on the leakage inductance Lk and magnetizing inductor Lm, the voltages of L_k and Lm are found as

$$V_{L_m} = DkV_{in}/(1-D) \tag{4}$$

$$V_{L_k} = D(1-k)(N+1)V_{in}/(2(1-D)) \tag{5}$$

$$V_{N_3} = NDkV_{in}/(1-D) \tag{6}$$

The voltages of capacitors C_1, C_2, C_3, and C_4 can be expressed as

$$V_{C_3} = NDkV_{in}/(1-D) \tag{7}$$

$$V_{C_1} = V_{C_2} = V_{L_k} + V_{L_m} = \frac{V_{in}D((1+k)+N(1-k))}{2(1-D)} \tag{8}$$

$$V_{C_4} = V_{in} + V_{C_1} + V_{C_3} + V_{N_3}$$

$$= \frac{2+Dk+DN-DNk-D+2Nk}{2(1-D)}V_{in} \tag{9}$$

According to (7)–(9), collecting the terms, the voltage gain can be expressed as

$$G_k = \frac{V_o}{V_{in}} = \frac{V_{C_1}+V_{C_2}+V_{C_3}+V_{C_4}+V_{in}}{V_{in}}$$

$$= \frac{2+Nk}{1-D} + \frac{D(N(1.5-0.5k)+(1.5k-0.5))}{1-D} \tag{10}$$

$$G = \frac{V_o}{V_{in}} = \frac{2+N}{1-D} + \frac{D(N+1)}{1-D} \tag{11}$$

$$V_{S1} = V_{S2} = V_{D1} = V_{D2} = \frac{V_{in}}{1-D} = \frac{V_o}{2+N+(N+1)D} \tag{12}$$

$$V_{D4} = \frac{NV_{in}}{1-D} = NV_o/(2+N+(N+1)D) \tag{13}$$

$$V_{D3} = V_{Do} = \frac{(N+1)V_{in}}{1-D} = \frac{(N+1)V_o}{2+N+(N+1)D} \tag{14}$$

$$I_{Do(t_2,t_8)} = I_o/(1-D) \tag{15}$$

$$I_{D1(t_2,t_7)} = I_{D2(t_2,t_7)} = I_o/D_c \tag{16}$$

Then, based on the capacitor charge balance, during the time interval $[t_0, t_2]$, the average current of capacitorC1can be written as

$$I_{C1[t_0,t_2]} = I_o/D \tag{17}$$

Therefore, the currents of secondary-side N_3 of the coupled inductor can be obtained

$$I_{N3[t_0,t_2]} = I_o/D \tag{18}$$

$$I_{N3[t_2,t_8]} = I_o/(1-D) \tag{19}$$

During the time interval $[t_2, t_8]$, while using KCL, at junction points of the primary side $N_1$of the coupled inductor, diode D_1 and capacitor C_4, the average current of the leakage inductor can be expressed

International Journal for Innovative Engineering and Management Research
A Peer Revieved Open Access International Journal
www.ijiemr.org

$$I_{L_k[t_2,t_8]} = (N+3)\,I_o/\left(2\,(1-D)\right) \tag{20}$$

$$N_1 I_{N1[t_0,t_2]} + N_2 I_{N2[t_0,t_2]} - N_3 I_{N3[t_0,t_2]} = N_1 I_{N1[t_2,t_8]} + N_2 I_{N2[t_2,t_7]} + N_3 I_{N3[t_2,t_8]}. \tag{21}$$

$$I_{N1[t_0,t_2]} = I_0\left(2D+N+DN\right)/\left(2D\left(1-D\right)\right) \tag{22}$$

Then, the RMS values of the switches S_1 and S_2 are

$$I_{\mathrm{RMS-S_1}} = \sqrt{\frac{1}{T_S}\int_0^{DT_S}\left(I_{N1[t_0,t_2]} + \frac{I_0}{D} - 0.5\Delta I_L + \frac{\Delta I_L}{DT_S}t\right)^2}$$

$$\mathrm{d}t = \sqrt{\frac{(2D+N+DN)^2}{4D(1-D)^2}I_0\left(\frac{K^2}{12}+1\right) + I_0\frac{2D+N+DN}{D(1-D)} + \frac{I_0^2}{D}}$$

$$I_{\mathrm{RMS-S_2}} = \sqrt{\frac{1}{T_S}\int_0^{DT_S}\left(I_{[t_0,t_2]} - 0.5\Delta I_L + \frac{\Delta I_L}{DT_S}t\right)^2}$$

$$\mathrm{d}t = \frac{2D+N+DN}{2D\,(1-D)}I_o\sqrt{D}\sqrt{\frac{K^2}{12}+1} \tag{23}$$

$$M = \frac{\frac{2+N+D(N+1)}{1-D} - \frac{5V_D}{V_{\mathrm{in}}}}{1 + R_L A + R_{DS}B + \frac{(4R_D+(4N+6)R_L)}{R(1-D)} + \frac{R_D+NR_L}{RD}} \tag{24}$$

Where

$$A = (N+ND+3D)(N+ND+2D)\Big/\left(RD(1-D)^2\right)$$

$$B = (N+ND+D+1)(N+ND+2D+1)/(RD(1-D))$$

$$\eta = \frac{2+N+D(N+1) - \frac{5V_D}{V_{\mathrm{in}}}(1-D)}{\left(1+R_L A + R_{DS}B + \frac{(4R_D+(4N+6)R_L)}{R(1-D)} + \frac{R_D+NR_L}{RD}\right)(2+N+D(N+1))} \tag{25}$$

IV. MATLAB/SIMULINK RESULTS

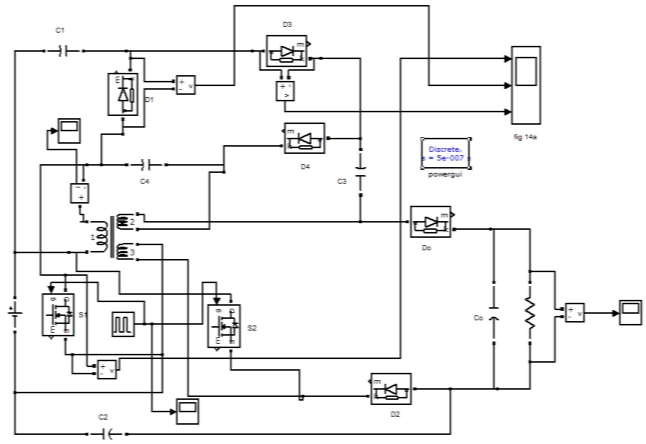

Fig.5 shows the matlab/Simulink model of proposed system

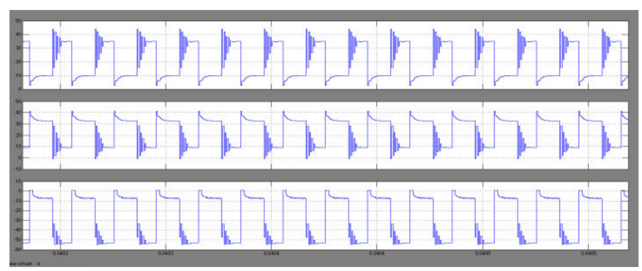

Fig.6 shows the simulation waveforms of proposed system like diode voltages and switch voltages.

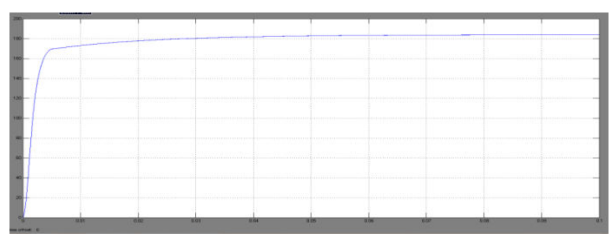

Fig.7 shows the output voltage of proposed converter

International Journal for Innovative Engineering and Management Research
A Peer Revieved Open Access International Journal
www.ijiemr.org

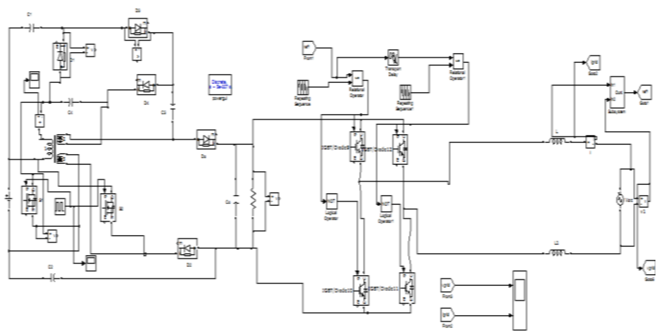

Fig.8 shows the proposed converter with grid connected system

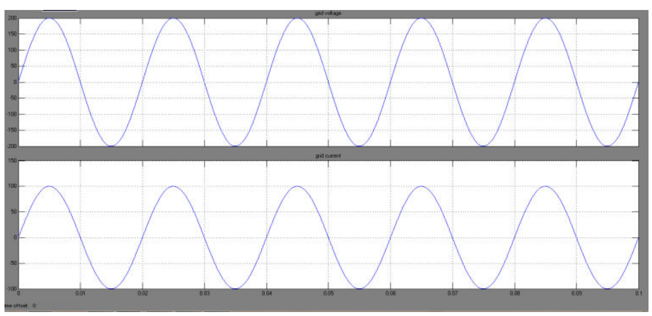

Fig.9 shows the grid outputs of grid voltage and gris current

V. CONCLUSION

The paper introduces closed loop control of high step up dual switch converter with coupled inductor and voltage multiplier cell for secondary grid connected applications. An additional control freedom is provided by the voltage multiplier cell to achieve extremely high voltage conversion ratio and to minimize the current ripple. The energy stored in the leakage inductance of the coupled inductor is recycled by using switched capacitors. The voltage stress across the main switch is reduced. Here the gate signals are generated using PWM control schemes. The proposed converter operated under open-loop & closed loop manner. The proposed converter has successfully implemented an efficient high step-up conversion through the voltage multiplier module. The interleaved structure reduces the input current ripple and distributes the current through each component. In addition, the lossless passive clamp function recycles the leakage energy and constrains a large voltage spike across the power switch. Meanwhile, the voltage stress on the power switch is restricted and much lower than the output voltage.

REFERENCES

[1]. Moumita Das and Vivek Agarwal, Student Member, IEEE, “Design and Analysis of a High efficiency DC-DC Converter with Soft Switching Capability for Renewable energy Applications Requiring High Voltage Gain” IEEE Trans. Ind. Electron., vol .63, NO. 5, May 2016.

[2]. W. Li and X. He, “Review of non-isolated high-step up DC/DC converters in photovoltaic grid connected applications,” IEEE Trans. Ind. Electron., vol. 58, no. 4, pp. 1239–1250, Apr. 2011.

[3]. K. W. Ma and Y. S. Lee, “An integrated fly-back converter for DC uninterruptible power supply,” IEEE Trans. Power Electron., vol. 11, no. 2,pp. 318– 327, Mar. 1996.

[4]. Q. Zhao and F. C. Lee, “High-efficiency, high step-up DC–DC converters,” IEEE Trans. Power Electron., vol. 18, no. 1, pp. 65–73, Jan.2003

[5]. G. C. Silveira, F. L. Tofoli, L. D. S. Bezerra, and R. P. Torrico-Bascope, “A non-isolated dc–dc boost converter with high voltage gain and balanced output voltage,”

IEEE Trans. Ind. Electron., vol. 61, no. 12, pp. 6739–6746, Dec. 2014.
[6]. C. T. Pan, C. F. Chuang, and C. C. Chu "A novel transformer-less adaptable voltage quadrupler DC converter with low switch voltage stress," IEEE Trans. Power Electron., vol. 29, no. 9, pp. 4787– 4796, Sep.2014.
[7]. P. Xuewei and A. K. Rathore, "Novel bidirectional snubberless naturally commutated soft-switching current-fed full-bridge isolated DC/DC converter for fuel cell vehicles," IEEE Trans. Ind. Electron., vol. 61, no. 5,pp. 2307–2315, May 2014.
[8]. C. T. Choi, C. K. Li, and S. K. Kok, "Modeling of an active clamp discontinuous conduction mode flyback converter under variation of operating conditions," in Proc. IEEE Int. Power Electron. Drive Syst. (PEDS), 1999, vol. 2, pp. 730–733.
[9]. M. Prudente, L. L. Pfitscher, G. mmendoerfer, E. F. Romaneli, and R. Gules, "Voltage multiplier cells applied to non-isolated DC–DC converters," IEEE Trans. Power Electron., vol. 23, no. 2, pp. 871–887, Mar. 2008.
[10]. J. Xu, "Modeling and analysis of switching DC–DC converter with coupled-inductor," in Proc. IEEE Int. Conf. Circuits Syst. (CICC), May 12–15, 1991, pp. 717–720.
[11]. A. F. Witulski, "Introduction to modeling of transformers and coupled inductors" IEEE Trans. Power Electron., vol. 10, no. 3, pp. 349–357, May 1995.
[12]. F. S. Garcia, J. A. Pomilio, and G. Spiazzi, "Modeling and control design of the interleaved double dual boost converter," IEEE Trans. Ind. Electron., vol. 60, no. 8, pp. 3283–3290, Aug. 2013.
[13]. P.W. Lee, Y. S. Lee, D. K.W. Cheng, and X. C. Liu, "Steady-state analysis of an interleaved boost converter with coupled inductors," IEEE Trans. Ind. Electron., vol. 47, no. 4, pp. 787–795, Aug. 2000. [14]. M. Kwon and B. H. Kwon, "High step-up active clamp converter with input-current doubler and output-voltage doubler for fuel cell power systems," IEEE Trans. Power Electron., vol. 24, no. 1, pp. 108–115, Jan. 2009.
[15]. K. C. Tseng and C. C. Huang, "High step-up high efficiency interleaved converter with voltage multiplier module for renewable energy system," IEEE Trans. Ind. Electron., vol. 61, no. 3, pp. 1311– 1319, Mar.2014.

AUTHORS PROFILE:

M.CHANDRA SHEKHAR completed his B.Tech in Electrical and Electronics Engineering from PRRM Engineering College (JNTUH), Shabad in the year 2005 and received M.Tech in the stream of Power Electronics Engineering at Auroras Engineering college(JNTUH),Bhongir, Nalgonda Dist, in the year 2012. Pursuing PhD in veltech Dr.RR& Dr.SR University Chennai. Currently working as a Assistant Professor in Annamacharya Inst of Tech & Sciences, Hyderabad, since 2012. And his areas of Interests are micro grid and renewable energy sources.

G.RADHAKRISHNA received B.Tech in Electrical and Electronics Engineering from Nalgonda Institute of Technology & Science(JNTUH) in the year 2013 and now pursuing M.Tech in the stream of Power Electronics Engineering at Annamacharya Inst. Of Tech.& Sciences,Hyderabad.

MR. JADAPALLI SREEDHAR was born at Rajampet near kadpa(dist.),AP., India. He completed his B.Tech in Electrical and Electronics Engineering, from JNTU in the year 2002. He completed his M.Tech in Power Electronics from JNTU in the year 2006. Currently, he is pursuing PhD from GITAM University, Hyderabad campus on the topic 'Synchronous Buck Converter Applications'. He is working as Associate Professor in the Department of EEE, Annamacharya Inst. Of Tech.& Sciences, Hyderabad, since 2012. His fields of interest are Power Systems and Power Electronics. So far, he has published 4 papers in International Journals and 1 paper in a National Journal.